Published as: *Cancer Res*. 2009 September 1; 69(17): 6782–6789.

Identification of a protein, G0S2, that lacks Bcl-2 homology domains and interacts with and antagonizes Bcl-2

Christian Welch[1], **Manas K. Santra**[1], **Wissal El-Assaad**[2], **Xiaochun Zhu**[1], **Wade E. Huber**[1], **Richard A. Keys**[1], **Jose G. Teodoro**[2], and **Michael R. Green**[1]

[1] Howard Hughes Medical Institute, Programs in Gene Function and Expression and Molecular Medicine, University of Massachusetts Medical School, Worcester, Massachusetts

[2] Goodman Cancer Center and Department of Biochemistry, McGill University, Montreal, Quebec

Abstract

The Bcl-2 family of proteins consists of both anti-apoptotic and pro-apoptotic factors, which share sequence homology within conserved regions known as Bcl-2 homology (BH) domains. Interactions between Bcl-2 family members, as well as with other proteins, regulate apoptosis through control of mitochondrial membrane permeability and release of cytochrome c. Here we identify a novel regulator of apoptosis that lacks BH domains but acts by binding Bcl-2 and modulating its anti-apoptotic activity. To identify regulators of apoptosis, we performed expression profiling in human primary fibroblasts treated with tumor necrosis factor alpha (TNFα), a potent inflammatory cytokine that can regulate apoptosis and functions, at least in part, by inducing expression of specific genes through NF-κB. We found that the gene undergoing maximal transcriptional induction following TNFα treatment was *G0/G1 switch gene 2* (*G0S2*), whose activation also required NF-κB. We show that *G0S2* encodes a mitochondrial protein that specifically interacts with Bcl-2 and promotes apoptosis by preventing the formation of protective Bcl-2/Bax heterodimers. We further demonstrate that ectopic expression of *G0S2* induces apoptosis in diverse human cancer cell lines in which endogenous *G0S2* is normally epigenetically silenced. Our results reveal a novel pro-apoptotic factor that is induced by TNFα through NF-κB, and which interacts with and antagonizes Bcl-2.

Keywords

apoptosis; Bcl-2; G0S2; NF-κB; TNFα

Introduction

Apoptosis has been implicated in a variety of biological processes including normal development, tissue homeostasis, and defense against pathogens (reviewed in ref. 1). Over the past decade, interest in apoptotic mechanisms has been greatly stimulated by the discovery that deregulation of cell death contributes to a number human pathologies including cancer, autoimmune disorders and degenerative diseases (reviewed in refs. 2,3).

A key component of the apoptotic machinery is a proteolytic system involving a family of cysteine proteases called caspases. Two pathways leading to caspase activation have been characterized: the extrinsic pathway, which involves so-called “death receptors”, and the intrinsic pathway, which involves the release of pro-apoptotic proteins from the mitochondria.

Requests for reprints: Michael Green, Program in Gene Function and Expression, University of Massachusetts Medical School, 364 Plantation Street, Worcester, MA, 01605. Phone: 508-856-5330; Fax: 508-856-5473; michael.green@umassmed.edu.

Commitment to apoptosis is governed by proteins of the Bcl-2 family, which are defined by the inclusion of one or more Bcl-2 homology (BH) domains (reviewed in refs. 2,4). The BH3 domain, for example, is a potent “death domain” that is critical for heterodimerization with other Bcl-2 family proteins. The Bcl-2 family includes both anti-apoptotic members, such as Bcl-2 and Bcl-xL, and pro-apoptotic members that either resemble Bcl-2 (e.g., Bax and Bak) or bear only the BH3 interaction domain (e.g., Bid, Bad, Bim, Noxa and Puma). Although the precise mechanism by which Bcl-2 proteins function is under investigation, it is clear that they regulate the release of proteins from the mitochondria that induce apoptosis.

A well-studied example of the extrinsic pathway is that induced by the inflammatory cytokine, tumor necrosis factor alpha (TNFα) (reviewed in ref. 5). TNFα promotes apoptosis through binding to its cell surface receptor, TNFR1, leading to the activation of downstream signal transduction pathways. Signaling through TNFR1 elicits rapid activation of two major heterodimeric transcription factors, AP-1 (also called c-Jun) and NF-κB.

NF-κB can either inhibit or induce apoptosis depending on cell type, extent of NF-κB activation, and nature of the apoptotic signal (reviewed in ref. 6). For example, NF-κB has been shown to antagonize TNFα-induced apoptosis by activating survival factors such as caspase-8-c-FLIP (FLICE inhibitory protein), cellular inhibitors of apoptosis (IAPs) and TNFR-associated factors TRAF1 and TRAF2. NF-κB also up-regulates several anti-apoptotic Bcl-2 family members and inhibits the intrinsic mitochondrial-dependent apoptosis pathway following DNA damage. By contrast, NF-κB can promote cell death, for example, when cells are cultured under conditions of serum withdrawal or treated with UV irradiation. Consistent with the ability of NF-κB to exhibit both pro- and anti-apoptotic activities, NF-κB does not always function as an oncogene and in some cases can act as a tumor suppressor (6).

Based upon these considerations we hypothesized the existence of novel, NF-κB dependent TNFα-inducible modulators of apoptosis. Here we perform expression profiling in human primary fibroblasts to identify new TNFα target genes that encode regulators of apoptosis.

Materials and Methods

Expression profiling

Early (<10) passage PFFs (ATCC) were treated with 25 ng/ml TNFα or PBS for 16 h, and poly $(A)^+$ mRNA was isolated using an Oligotex Direct mRNA Midi Kit (Qiagen). 2 μg of mRNA was used to generate cDNA using an oligo(dT) T7 primer and Superscript cDNA Synthesis Kit (Invitrogen). The cDNA was *in vitro* transcribed using the T7 Megascript Kit (Ambion). The resulting cRNA was fragmented by heating at 94°C for 30 min and hybridized against Affymetrix Hu6800 and Hu35K microarrays, which were scanned and analyzed using Affymetrix Microarray Suite software. Raw data have been submitted to the Array Express repository.

G0S2 expression analysis

For northern blots, 1 μg poly(A)+ mRNA was loaded per lane and hybridized with a random primer-labeled probe for *G0S2* or *GAPDH*. For immunoblotting, PFFs were treated with TNFα and 16 h later, whole cell extracts were made by lysing cells in 1X Laemmli buffer. Blots were probed with a G0S2 rabbit polyclonal antibody (generated by Covance Laboratories by immunizing rabbits with purified, recombinant His-tagged G0S2 produced in *E. coli*) or tubulin monoclonal antibody (Sigma) followed by the appropriate HRP-conjugated α-Ig secondary antibody (Amersham Biosciences).

RT-PCR analysis

PFFs were infected with Ad-LacZ or Ad-IκB-SR and treated with TNFα (25 ng/ml) or PBS. 24 h later, total RNA was isolated using TRIzol Reagent (Invitrogen) and used to perform RT-PCR. For the demethylation experiments, cells were treated with AZA and TSA as previously described (7).

Plasmid and adenovirus construction

G0S2 was cloned by RT-PCR amplification using poly(A)+ mRNA isolated from TNFα-treated PFFs. The PCR product, including the sequence for the HA epitope, was subcloned into pcDNA3 (Invitrogen) to generate pcDNA-G0S2-HA. Plasmids expressing EGFP-G0S2 and G0S2-EYFP were derived by subcloning the G0S2 sequence from pcDNA3-G0S2-HA into pEGFP-C1 (Clontech) or pEYFP (Clontech), respectively. To generate GFP-tagged G0S2 deletion mutants, truncated G0S2 sequences were PCR amplified and cloned into pEGFP-C1. Point mutations in G0S2 were generated using the Quick Change Mutagenesis Kit (Stratagene) using pcDNA3-G0S2-HA as the template. All clones were confirmed by restriction digest analysis and DNA sequencing.

To construct plasmids expressing N-terminal FLAG-tagged Bcl-2 family members, the corresponding cDNAs (obtained from Stanley Korsmeyer) were PCR amplified and cloned into p3XFLAG-myc-CMV-26 (Sigma). To construct the plasmid expressing Bax-V5, Bax cDNA was PCR amplified and cloned into pcDNA4-V5/V5HisA (Invitrogen). Plasmids expressing Bcl-2-ECFP and Bad-ECFP were generated by cloning PCR-amplified cDNAs into pECFP-C1.

Adenovirus vectors expressing wild-type G0S2 (Ad-G0S2) or the G0S2 (R57A, D58A) mutant, both containing a single HA epitope at the C-terminus, were generated using the AdEasy XL Adenoviral Vector System (Stratagene). Adenovirus vectors Ad-LacZ (8) and Ad-IκB-SR (9) have been previously described. Target cells were infected with adenovirus vectors at ~80% confluence at an MOI of 35 pfu/cell.

Immunofluorescence and fluorescence microscopy

H1299 cells (ATCC) were transfected using Fugene 6 transfection reagent (Roche). 36 h later cells were fixed in 4% paraformaldehyde (in PBS), permeabilized in 0.5% TritonX-100 (in PBS) and stained with an α-HA monoclonal antibody (Sigma) followed by α-mouse Ig Texas Red-conjugated secondary antibody (Jackson Laboratories), or Mitotracker (Molecular Probes/Invitrogen). Cells were visualized with a Zeiss Axiophot2 fluorescence microscope using Axiovision 3.1 software.

Biochemical fractionation

Mitochondria were isolated from TNFα-treated PFFs using The ApoAlert Cell Fractionation Kit (Clontech). Immunoblotting was performed using antibodies to G0S2, Aurora A (Novus Biologicals) and COX IV (BD-Clontech).

Co-immunoprecipitations

For co-transfection experiments, ~2×10^7 cells were co-transfected with appropriate plasmids and 24 h later cells were harvested and lysed in 1% CHAPS buffer as previously described (10). Following centrifugation, supernatants were incubated with 20 μl equilibrated EZview Redα-HA beads or α-Flag M2 affinity beads (Sigma) for 4 h at 4°C. Beads were washed three times in 1% CHAPS buffer and bound proteins were eluted. Immunoprecipitated material and whole cell extracts were blotted and probed with α-FLAG M2 (Sigma),α-HA (Sigma),α-EGFP (Clontech) or α-V5 (Invitrogen) monoclonal antibodies. For adenovirus experiments, HeLa

cells (ATCC) were infected and 24 h later mitochondria were isolated as described above and lysed in 1% CHAPS buffer. G0S2 was immunoprecipitated using EZview Red α-HA beads, and immunoblotting was performed using α-Bcl-2 (BD Pharmingen) and α-HA monoclonal antibodies.

GST pull-down assays

In vitro translation of G0S2 was performed using the T7 TnT Quick Coupled *In Vitro* Translation System (Invitrogen) using the plasmid pcDNA3-G0S2-HA. The GST-Bcl-2 fusion protein, in which the N-terminal domain (amino acids 1–20) of Bcl-2 was deleted, was expressed in *E. coli* from pGEX-4T-1 (Amersham) as previously described (11). 1 μg of GST or GST-Bcl-2 immobilized on 10 μl glutathione-Sepharose was incubated with 10 μl *in vitro* translated G0S2 for 4 h at 4° C in GST lysis buffer. Pull-downs were washed four times with lysis buffer (50 mM Tris pH 7.5, 150 mM NaCl, 1 mM EDTA, 0.5 mM DTT, 0.05% Triton X-100), analyzed by SDS-PAGE and visualized using a Fujifilm FLA-5000 PhosphorImager system.

Fluorescence resonance energy transfer

Twenty-four hours after co-transfection, HCT116 cells (ATCC) were transferred to poly-lysine coated glass slides, and examined using a Leica confocal laser scanning microscope system (TCS SP2 AOBS; Leica Microsystems). The 458 nm laser-line was used to excite the focused cells, and the images were captured with a liquid-cooled CCD camera. Digitized microscope images were analyzed to select a region of interest (ROI) in a single cell to optimize the signal-to-noise ratio. Spectra were recorded from three cells and the spectra averaged and plotted. To record ECFP emission spectra, the ECFP donor in the selected ROI of a single cell was excited with the 405 nm laser-line to avoid leak-through of ECFP emission over EYFP emission, and emission spectra were generated by scanning the ROI eight times with 10 nm spectral resolution and recorded using Leica Confocal Software (LCS). To record EYFP emission spectra, the EYFP-fluorophore was excited by the 488 nm laser-line.

Apoptosis assays

Cells were stained using the Annexin V-PE Apoptosis Detection Kit-I (BD Pharmingen) and analyzed using a Guava Personal flow cytometer (Guava Technologies, Inc). UV treatment of HeLa/Bcl-2 and HeLa/Neo cells (generated by stable transfection with plasmids expressing FLAG-Bcl-2 or empty vector [p3XFLAG-myc-CMV-26; Sigma)] was performed by irradiating cells for 30 sec in a UV Stratalinker (Stratagene). For luciferase-based assays, H1299 cells were co-transfected with pcDNA3-Luciferase (12) and appropriate plasmids. For experiments in primary cells, PFFs were treated with camptothecin in the presence or absence of TNFα (25 ng/ml). After 72 h, cells were trypsinized, washed with cold PBS three times, stained and analyzed as described above.

RNA interference

PFF cells were stably transduced with a G0S2 shRNA (source location V2LHS-114719) or a non-silencing shRNA (5′-TCTCGCTTGGGCGAGAGTAAG-3′), obtained from Open Biosystems.

Analysis of *G0S2* expression in tumor samples

Human samples of normal lung, adenocarcinoma and squamous cell carcinoma were obtained from the UMass Cancer Center Tissue Bank. Gene expression levels were analyzed by qRT-PCR using Platinum SYBR Green qPCR SuperMix-UDG with Rox (Invitrogen) and the following primers: *G0S2* (forward, 5′-GGCCTGATGGAGACTGTGTG-3′ and reverse, 5′-CTTGCTTCTGGAGAGCCTGT-3) and *GAPDH* (forward, 5′-

TGCACCACCAACTGCTTAGC-3′ and reverse, 5′-GGCATGGACTGTGGTCATGAG-3′). For each sample, *GAPDH* provided an internal normalization control. The average *G0S2* expression level in the 10 normal samples was assigned as 1.

Results

Identification of *G0S2* as an NF-κB-dependent downstream target of the TNFα pathway

To identify transcriptional targets downstream of TNFα, we used high-density cDNA microarrays to compare the expression profiles of human primary foreskin fibroblasts (PFFs) treated in the presence or absence of TNFα. Of the 33,000 genes represented on the microarray, 138 showed increased expression and 27 showed decreased expression by 4-fold or more upon TNFα treatment (Supplementary Table S1). As expected, this approach identified numerous genes known to be induced by TNFα including *TNFAIP2*, *TNFAIP3* and *TNFAIP6* (13), as well as *VCAM1* (14) and *PTSG2* (also known as *COX2*) (15).

The gene most highly induced following TNFα treatment was *G0/G1 switch 2* (*G0S2)*, which encodes a protein of unknown function. Northern blot analysis indicated that *GOS2* is widely expressed in normal human tissues and is present at particularly high levels in peripheral blood, skeletal muscle and heart (Supplementary Fig. S1).

To verify the results of the microarray experiment, we analyzed *GOS2* mRNA and protein levels in PFFs following TNFα treatment. The northern blot of Fig. 1*A* (left panel) confirms that *G0S2* was transcriptionally up-regulated in PFFs following TNFα treatment. Quantitative RT-PCR (qRT-PCR) analysis indicated that *G0S2* induction could be detected as early as 1 hour and reached maximal levels by 4 hours following TNFα treatment (Supplementary Fig. S2). Immunoblot analysis showed that, like mRNA levels, G0S2 protein levels were also up-regulated in PFFs following TNFα treatment (Fig. 1*A*, right panel).

To determine whether TNFα-mediated induction of *G0S2* was dependent upon NF-κB, we monitored *G0S2* expression in cells infected with an adenovirus expressing a super repressor form of IκB (Ad-IκB-SR), which blocks NF-κB activation (16,17). The RT-PCR analysis of Fig. 1*B* shows that *G0S2* induction by TNFα was abrogated in PFFs expressing Ad-IκB-SR but not a control adenovirus expressing LacZ (Ad-LacZ). Collectively, these results indicate that *G0S2* is induced by TNFα through activation of NF-κB.

TNFα also induced expression of *cIAP1* and *cIAP2*, two known NF-κB target genes (18), with kinetics comparable to that of *G0S2*, whereas expression of another reported NF-κB target gene, *Bcl-xL* (19), was not induced by TNFα treatment (Supplementary Fig. S2).

G0S2 is a mitochondrial protein

As a first step toward elucidating the function of G0S2, we determined its subcellular localization. H1299 non-small cell lung cancer cells were transfected with a plasmid encoding a C-terminal hemagglutinin (HA)-tagged version of G0S2 (G0S2-HA) and the protein was detected by indirect immunofluorescence using an α-HA antibody. Fig. 1*C* (top left panel) shows that G0S2-HA displayed a staining pattern that was characteristic of the mitochondria, which was confirmed by co-localization with the mitochondrial dye Mitotracker (Fig. 1*C*, top middle and right panels). The localization pattern was not a consequence of the C-terminal epitope tag, as an N-terminal enhanced green fluorescent protein (EGFP)-tagged version of G0S2 also localized to the mitochondria (Fig. 1*C*, bottom panels). Biochemical fractionation experiments and subsequent immunoblot analysis using an α-G0S2 antibody confirmed that endogenous G0S2 was present in the mitochondria (Fig. 1*D*).

G0S2 directly interacts with the anti-apoptotic protein Bcl-2

The mitochondrial localization of G0S2, in conjunction with the well-established role of NF-κB in apoptosis, prompted us to test whether G0S2 interacts with one or more members of the Bcl-2 family. HEK293 embryonic kidney cells were co-transfected with plasmids expressing G0S2-HA and a FLAG-tagged Bcl-2 family member. G0S2-HA was immunoprecipitated using an α-HA antibody and the immunoprecipitate was analyzed for the Bcl-2 family member by immunoblotting with an α-FLAG antibody. Fig. 2*A* shows that of the proteins tested, only Bcl-2 was readily detectable in the G0S2 immunoprecipitate. Significantly weaker interactions were also detected between G0S2 and the anti-apoptotic proteins Bcl-xL and Mcl-1, which were evident only upon overexposure of the autoradiogram (data not shown).

To confirm the association between G0S2 and Bcl-2, HeLa cells were infected with Ad-G0S2 (in which G0S2 was epitope-tagged at the C-terminus with HA), and G0S2 was immunoprecipitated from the mitochondrial fraction using an α-HA antibody and the immunoprecipitate was analyzed for endogenous Bcl-2 using an α-Bcl-2 antibody. Fig. 2*B* shows that Bcl-2 was present in the immunoprecipitate from Ad-G0S2-infected cells but not from control cells infected with Ad-LacZ. *In vitro* GST pull-down assays using purified GST-tagged Bcl-2 and *in vitro* translated ^{35}S-methionine labeled G0S2 confirmed that the interaction between G0S2 and Bcl-2 was direct (Fig. 2*C*).

Finally, to determine whether G0S2 directly interacted with Bcl-2 *in vivo*, we used a fluorescence resonance energy transfer (FRET) assay. Plasmids expressing enhanced cyan fluorescence protein (ECFP) fused to the C-terminus of Bcl-2 or Bad (Bcl-2-ECFP or Bad-ECFP, respectively) and enhanced yellow fluorescence protein (EYFP) fused to the C-terminus of G0S2 (G0S2-EYFP) were transiently transfected into HCT116 colorectal cells in pairwise combinations, and the cell lines were analyzed by FRET. The results of Fig. 2*D* show that a FRET signal was observed in cells expressing Bcl-2-ECFP and G0S2-EYFP, consistent with the results of Figs. 2*A*–*C*, but not in cells expressing Bad-ECFP and G0S2-EYFP. Collectively, the results of Fig. 2 indicate that G0S2 directly interacts with Bcl-2 both *in vitro* and *in vivo*.

G0S2 induces apoptosis in transformed cells dependent upon interaction with Bcl-2

The above findings raised the possibility that G0S2 could have pro- or anti-apoptotic activity. We therefore tested whether ectopic expression of G0S2 could induce apoptosis in transformed cells. H1299 and HCT116 cells were infected with Ad-G0S2 or Ad-LacZ, and 36 hours later stained with Annexin V-PE. Fig. 3*A* shows that in both cell lines expression of Ad-G0S2 induced pronounced apoptosis, whereas little or no cell death was observed in Ad-LacZ or mock-infected cells. G0S2 expression and induction of apoptosis could be detected by 20 hours post-infection and the level of apoptosis increased over 72 hours (Supplementary Fig. S3).

To examine whether the ability of G0S2 to induce apoptosis and to interact with Bcl-2 were related activities, we sought to generate G0S2 mutants that were abrogated for their ability to interact with Bcl-2. We first delineated the region of G0S2 required for Bcl-2 interaction using a panel of G0S2 deletion mutants in which fragments of G0S2 were fused to the C-terminus of GFP (Fig. 3*B*, top panel). The co-immunoprecipitation experiments of Fig. 3*B* (bottom panel) show that only constructs harboring the central region of G0S2 (amino acids 33 to 67) interacted with Bcl-2.

We next constructed a series of point mutants in the central region by mutating pairs of amino acids to alanine (Fig. 3*C*, top). Fig. 3*C* shows that mutations in amino acids 35 to 46 retained association with Bcl-2 at a level comparable to that of wild-type G0S2 protein. However, mutations in amino acids 50 to 58 reduced interaction with Bcl-2; in particular, the G0S2 mutant

derivative in which arginine-57 and aspartic acid-58 were mutated to alanine (R57A, D58A) was dramatically reduced for Bcl-2 interaction.

We then tested whether the G0S2(R57A, D58A) mutant was impaired for apoptotic activity. H1299 cells were infected with an adenovirus expressing wild-type G0S2 or the G0S2(R57A, D58A) mutant, and apoptosis was monitored by staining with Annexin V-PE. Fig. 3*D* shows that the ability of G0S2(R57A, D58A) to induce apoptosis was significantly reduced compared to the wild-type protein. The reduced ability of G0S2(R57A, D58A) to interact with Bcl-2 and induce apoptosis was not a result of mislocalization of the protein, as the mutant protein retained mitochondrial localization (Supplementary Fig. S4). These results indicate that interaction with Bcl-2 is required for G0S2 to induce apoptosis.

G0S2 promotes apoptosis by preventing Bcl-2/Bax heterodimerization

We next investigated the mechanism by which G0S2 induces apoptosis. Bcl-2 mediates its survival function, at least in part, by heterodimerizing with Bcl-2 family members, such as Bax (20), and countering their pro-apoptotic activity. The co-immunoprecipitation experiment of Fig. 4*A* shows that addition of G0S2 inhibited the ability of Bcl-2 and Bax to co-immunoprecipitate, suggesting that G0S2 inhibits Bcl-2 function by preventing the formation of protective Bcl-2/Bax heterodimeric complexes.

A prediction of this model is that in the presence of G0S2, Bcl-2 would be unable to carry out its anti-apoptotic function. To test this idea, HeLa cells stably expressing either Bcl-2 (HeLa/Bcl-2) or, as a control, vector (HeLa/Neo), were infected with Ad-G0S2 or Ad-LacZ. Fig. 4*B* shows, as expected, that over-expression of Bcl-2 protected HeLa cells from UV-induced apoptosis (left panel) but failed to protect HeLa cells from G0S2-mediated apoptosis (right panel).

As an alternative experimental approach, we used a co-transfection strategy. In this experiment, apoptosis was monitored using an assay in which luciferase activity serves as a proxy for cell death (12). H1299 cells were co–transfected with plasmids expressing luciferase and, as an apoptotic stimulus, Bax. Fig. 4*C* shows, as expected, that expression of Bax alone induced cell death, as evidenced by a dramatic reduction in luciferase activity compared to that observed in cells transfected with empty vector. Co-expression of Bcl-2 and Bax prevented the reduction in luciferase activity, consistent with previous studies showing that expression of Bcl-2 can inhibit Bax-induced apoptosis (20,21). Significantly, expression of G0S2 together with Bax and Bcl-2 resulted in a level of luciferase activity comparable to that obtained upon expression of Bax alone, indicating the anti-apoptotic activity of Bcl-2 was inhibited. Collectively, the results of Fig. 4 indicate that G0S2 induces apoptosis by inhibiting the ability of Bcl-2 to form anti-apoptotic Bcl-2/Bax heterodimers.

G0S2 sensitizes primary cells to undergo apoptosis

The finding that *G0S2* could induce apoptosis in transformed cells prompted us to ask whether G0S2 also had a pro-apoptotic effect in primary cells. As has been observed in previous studies (see for example, refs. 16,22), we found that treatment of primary fibroblasts, such as PFFs, with TNFα did not induce apoptosis (see below). However, we tested whether TNFα treatment sensitized cells to apoptosis. Toward this end, PFFs were treated with a series of low concentrations of the DNA damaging agent camptothecin, a known inducer of apoptosis, in the presence or absence of TNFα. The results of Fig. 5*A* indicate that TNFα treatment resulted in increased apoptosis, indicating that the net effect of TNFα treatment is pro-apoptotic.

To determine whether G0S2 was responsible for the pro-apoptotic activity of TNFα we performed an RNA interference (RNAi) experiment. The results of Fig. 5*B* indicate that

shRNA-mediated knockdown of G0S2 (Supplementary Fig. S5) abrogated the ability of TNFα to increase the level of camptothecin-induced apoptosis. Thus, *G0S2* is a TNFα-inducible gene required for sensitizing PFFs to undergo apoptosis.

Finally, we asked whether ectopic expression of *G0S2* was sufficient to sensitize PFFs to undergo apoptosis. PFFs were infected with Ad-G0S2 or Ad-LacZ and 24 hours later challenged with various doses of camptothecin. The results of Fig. 5*C* show that ectopic expression of *G0S2* resulted in a higher level of apoptosis, whereas little or no cell death was observed in control Ad-LacZ-infected cells. Thus, G0S2 is sufficient to sensitize primary cells to undergo apoptosis in response to DNA damage.

The *G0S2* gene is epigenetically silenced in human cancer cell lines

Many genes that negatively regulate cell survival are epigentically silenced in human cancers through promoter hypermethylation (reviewed in ref. 23). Notably, the *G0S2* promoter contains a CpG-rich island (24), suggesting it may undergo epigenetic silencing. To test this hypothesis, we monitored *G0S2* expression in a panel of human cancer cell lines before and after treatment with the demethylating agent 5-aza-2′-deoxycytidine (AZA) and the histone deacetylase inhibitor trichostatin A (TSA). The RT-PCR results of Fig. 6*A* show that *G0S2* expression was induced by AZA/TSA treatment in all human cancer cell lines examined, but not in normal PFFs. Cell lines in which *G0S2* was highly induced were also analyzed for G0S2 protein by immunoblotting; as expected, in all cases AZA/TSA treatment resulted in a substantial increase in G0S2 protein levels (Figure 6*B*). These results indicate that the *G0S2* gene is epigenetically silenced in a variety of human cancer cell lines.

Several of the cell lines in which *G0S2* was epigenetically repressed were derived from non-small cell lung cancers. We therefore analyzed whether *G0S2* expression was down-regulated in a panel of non-small cell lung tumors. The qRT-PCR results of Fig. 6*C* indicate that *G0S2* expression was down-regulated greater than 5-fold in 70% of lung adenocarcinoma samples and 90% of lung squamous cell carcinoma samples analyzed. In addition, a search of the Oncomine cancer profiling database (25) revealed that *G0S2* was frequently down-regulated in a variety of other solid tumors (Supplementary Fig. S6).

Discussion

Here we have shown that the *G0S2* gene is induced in human primary cells by TNFα treatment in a manner that depends on NF-κB. Moreover, we found that *G0S2* induces apoptosis in human cancer cell lines and sensitizes primary cells to undergo apoptosis. G0S2 induces apoptosis by directly interacting with Bcl-2 and preventing its ability to heterodimerize with Bax.

We found that the *G0S2* gene is epigenetically silenced in a number of human cancer cell lines, and is down-regulated at high frequency in non-small cell lung cancers. Our results are consistent with those of a previous study, which found that the *G0S2* promoter is hypermethylated in approximately a third of primary head and neck squamous cell carcinomas (26). The pro-apoptotic activity of G0S2 and its epigenetic repression in tumors and human cancer cell lines raise the possibility that *G0S2* is a tumor suppressor gene. Consistent with this idea, we found that shRNA-mediated knockdown of G0S2 promoted oncogene-induced transformation (Supplementary Fig. S7).

Our results fit in well with several studies that have identified other TNFα-inducible pro-apoptotic NF-κB targets such as *TIEG* and *IEX*-1 (27,28). Interestingly, in some cell types activation of NF-κB is required to mediate toxicity of cancer therapeutic agents. For example, activation of NF-κB is required for cell death induced by doxorubicin and its analogs (29,30). Similarly, cellular resistance to vincristine has been shown to be mediated by inhibition of NF-

κB activation (31). Taken together, these data suggest that in some cancer types NF-κB activation may enhance the activity of conventional chemotherapies. It may therefore be beneficial to determine if silencing of *G0S2* correlates with low response of tumors to chemotherapy or poor patient outcome.

Supplementary Material

Refer to Web version on PubMed Central for supplementary material.

Acknowledgments

We thank Roger Davis, Stanley Korsmeyer, Frank Graham, Emmanuel Petroulakis, Nahum Sonenberg and Albert Baldwin Jr. for providing reagents and Sara Evans for editorial assistance. J.G.T. holds a Canadian Institute of Health Research (CIHR) New Investigator award and is a Chercheur-Boursier of the Fonds de la Recherche en Sante du Quebec (FRSQ). Research in the lab of J.G.T. is supported by a grant (MOP-86752) from the CIHR. M.R.G. is an investigator of the Howard Hughes Medical Institute.

References

1. Adams JM, Cory S. The Bcl-2 apoptotic switch in cancer development and therapy. Oncogene 2007;26:1324–37. [PubMed: 17322918]
2. Letai AG. Diagnosing and exploiting cancer's addiction to blocks in apoptosis. Nat Rev Cancer 2008;8:121–32. [PubMed: 18202696]
3. Cacciapaglia F, Spadaccio C, Chello M, et al. Apoptotic molecular mechanisms implicated in autoimmune diseases. Eur Rev Med Pharmacol Sci 2009;13:23–40. [PubMed: 19364083]
4. Danial NN. BCL-2 family proteins: critical checkpoints of apoptotic cell death. Clin Cancer Res 2007;13:7254–63. [PubMed: 18094405]
5. Bertazza L, Mocellin S. Tumor necrosis factor (TNF) biology and cell death. Front Biosci 2008;13:2736–43. [PubMed: 17981749]
6. Dutta J, Fan Y, Gupta N, Fan G, Gelinas C. Current insights into the regulation of programmed cell death by NF-kappaB. Oncogene 2006;25:6800–16. [PubMed: 17072329]
7. Cameron EE, Bachman KE, Myohanen S, Herman JG, Baylin SB. Synergy of demethylation and histone deacetylase inhibition in the re-expression of genes silenced in cancer. Nat Genet 1999;21:103–7. [PubMed: 9916800]
8. Bacchetti S, Graham FL. Inhibition of cell proliferation by an adenovirus vector expressing the human wild type 953 protein. Int J Oncol 1993;3:781–8.
9. Wang CY, Cusack JC Jr, Liu R, Baldwin AS Jr. Control of inducible chemoresistance: enhanced anti-tumor therapy through increased apoptosis by inhibition of NF-kappaB. Nat Med 1999;5:412–7. [PubMed: 10202930]
10. Hsu YT, Youle RJ. Nonionic detergents induce dimerization among members of the Bcl-2 family. J Biol Chem 1997;272:13829–34. [PubMed: 9153240]
11. Bruey JM, Bruey-Sedano N, Luciano F, et al. Bcl-2 and Bcl-XL regulate proinflammatory caspase-1 activation by interaction with NALP1. Cell 2007;129:45–56. [PubMed: 17418785]
12. Lei K, Nimnual A, Zong WX, et al. The Bax subfamily of Bcl2-related proteins is essential for apoptotic signal transduction by c-Jun NH(2)-terminal kinase. Mol Cell Biol 2002;22:4929–42. [PubMed: 12052897]
13. Dixit VM, Green S, Sarma V, et al. Tumor necrosis factor-alpha induction of novel gene products in human endothelial cells including a macrophage-specific chemotaxin. J Biol Chem 1990;265:2973–8. [PubMed: 2406243]
14. Osborn L, Hession C, Tizard R, et al. Direct expression cloning of vascular cell adhesion molecule 1, a cytokine-induced endothelial protein that binds to lymphocytes. Cell 1989;59:1203–11. [PubMed: 2688898]
15. Fournier T, Fadok V, Henson PM. Tumor necrosis factor-alpha inversely regulates prostaglandin D2 and prostaglandin E2 production in murine macrophages. Synergistic action of cyclic AMP on

cyclooxygenase-2 expression and prostaglandin E2 synthesis. J Biol Chem 1997;272:31065–72. [PubMed: 9388257]

16. Van Antwerp DJ, Martin SJ, Kafri T, Green DR, Verma IM. Suppression of TNF-alpha-induced apoptosis by NF-kappaB. Science 1996;274:787–9. [PubMed: 8864120]
17. Zandi E, Rothwarf DM, Delhase M, Hayakawa M, Karin M. The IkappaB kinase complex (IKK) contains two kinase subunits, IKKalpha and IKKbeta, necessary for IkappaB phosphorylation and NF-kappaB activation. Cell 1997;91:243–52. [PubMed: 9346241]
18. Stehlik C, de Martin R, Kumabashiri I, Schmid JA, Binder BR, Lipp J. Nuclear factor (NF)-kappaB-regulated X-chromosome-linked iap gene expression protects endothelial cells from tumor necrosis factor alpha-induced apoptosis. J Exp Med 1998;188:211–6. [PubMed: 9653098]
19. Chen C, Edelstein LC, Gelinas C. The Rel/NF-kappaB family directly activates expression of the apoptosis inhibitor Bcl-x(L). Mol Cell Biol 2000;20:2687–95. [PubMed: 10733571]
20. Oltvai ZN, Milliman CL, Korsmeyer SJ. Bcl-2 heterodimerizes in vivo with a conserved homolog, Bax, that accelerates programmed cell death. Cell 1993;74:609–19. [PubMed: 8358790]
21. Otter I, Conus S, Ravn U, et al. The binding properties and biological activities of Bcl-2 and Bax in cells exposed to apoptotic stimuli. J Biol Chem 1998;273:6110–20. [PubMed: 9497329]
22. Beg AA, Baltimore D. An essential role for NF-kappaB in preventing TNF-alpha-induced cell death. Science 1996;274:782–4. [PubMed: 8864118]
23. Robertson KD. DNA methylation and human disease. Nat Rev Genet 2005;6:597–610. [PubMed: 16136652]
24. Russell L, Forsdyke DR. A human putative lymphocyte G0/G1 switch gene containing a CpG-rich island encodes a small basic protein with the potential to be phosphorylated. DNA Cell Biol 1991;10:581–91. [PubMed: 1930693]
25. Rhodes DR, Yu J, Shanker K, et al. ONCOMINE: a cancer microarray database and integrated data-mining platform. Neoplasia 2004;6:1–6. [PubMed: 15068665]
26. Tokumaru Y, Yamashita K, Osada M, et al. Inverse correlation between cyclin A1 hypermethylation and p53 mutation in head and neck cancer identified by reversal of epigenetic silencing. Cancer Res 2004;64:5982–7. [PubMed: 15342377]
27. Osawa Y, Nagaki M, Banno Y, et al. Expression of the NF-kappa B target gene X-ray-inducible immediate early response factor-1 short enhances TNF-alpha-induced hepatocyte apoptosis by inhibiting Akt activation. J Immunol 2003;170:4053–60. [PubMed: 12682234]
28. Zhou A, Scoggin S, Gaynor RB, Williams NS. Identification of NF-kappa B-regulated genes induced by TNFalpha utilizing expression profiling and RNA interference. Oncogene 2003;22:2054–64. [PubMed: 12673210]
29. Ashikawa K, Shishodia S, Fokt I, Priebe W, Aggarwal BB. Evidence that activation of nuclear factor-kappaB is essential for the cytotoxic effects of doxorubicin and its analogues. Biochem Pharmacol 2004;67:353–64. [PubMed: 14698047]
30. Bian X, McAllister-Lucas LM, Shao F, et al. NF-kappa B activation mediates doxorubicin-induced cell death in N-type neuroblastoma cells. J Biol Chem 2001;276:48921–9. [PubMed: 11679590]
31. Giri DK, Pantazis P, Aggarwal BB. Cellular resistance to vincristine suppresses NF-kappa B activation and apoptosis but enhances c-Jun-NH2-terminal protein kinase activation by tumor necrosis. Apoptosis 1999;4:291–301. [PubMed: 14692400]

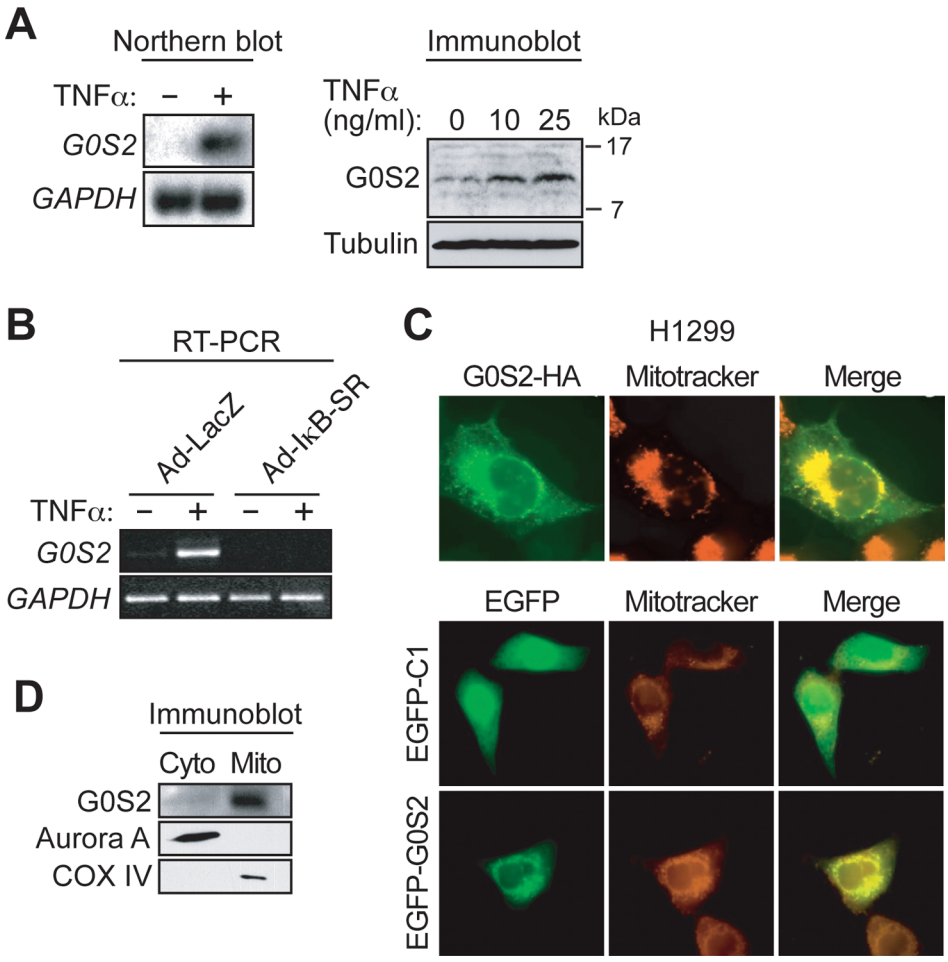

Figure 1.

G0S2 is an NF-κB-dependent downstream target of TNFα that encodes a mitochondrial protein. *A*, *G0S2* expression was analyzed by northern blot (left) or immunoblotting (right) in TNFα-treated PFFs. *GAPDH* and tubulin were monitored as loading controls. *B*, RT-PCR analysis monitoring *G0S2* expression in TNFα-treated PFFs infected with Ad-LacZ or Ad-IκB-SR. *C*, (Top) Immunofluorescence of G0S2-HA-expressing H1299 cells stained with an α-HA antibody (left) or Mitotracker (middle). Merged images are shown (right). (Bottom) Immunofluorescence of H1299 cells expressing EGFP-G0S2 or empty vector (EGFP-C1). Cells were visualized for GFP (left) or Mitotracker (middle). *D*, Biochemical fractionation. Whole cell extracts prepared from TNFα-treated PFF cells were separated into mitochondrial and cytoplasmic fractions and immunoblotted for G0S2, Aurora A (a cytoplasmic protein) or COX IV (a mitochondria marker).

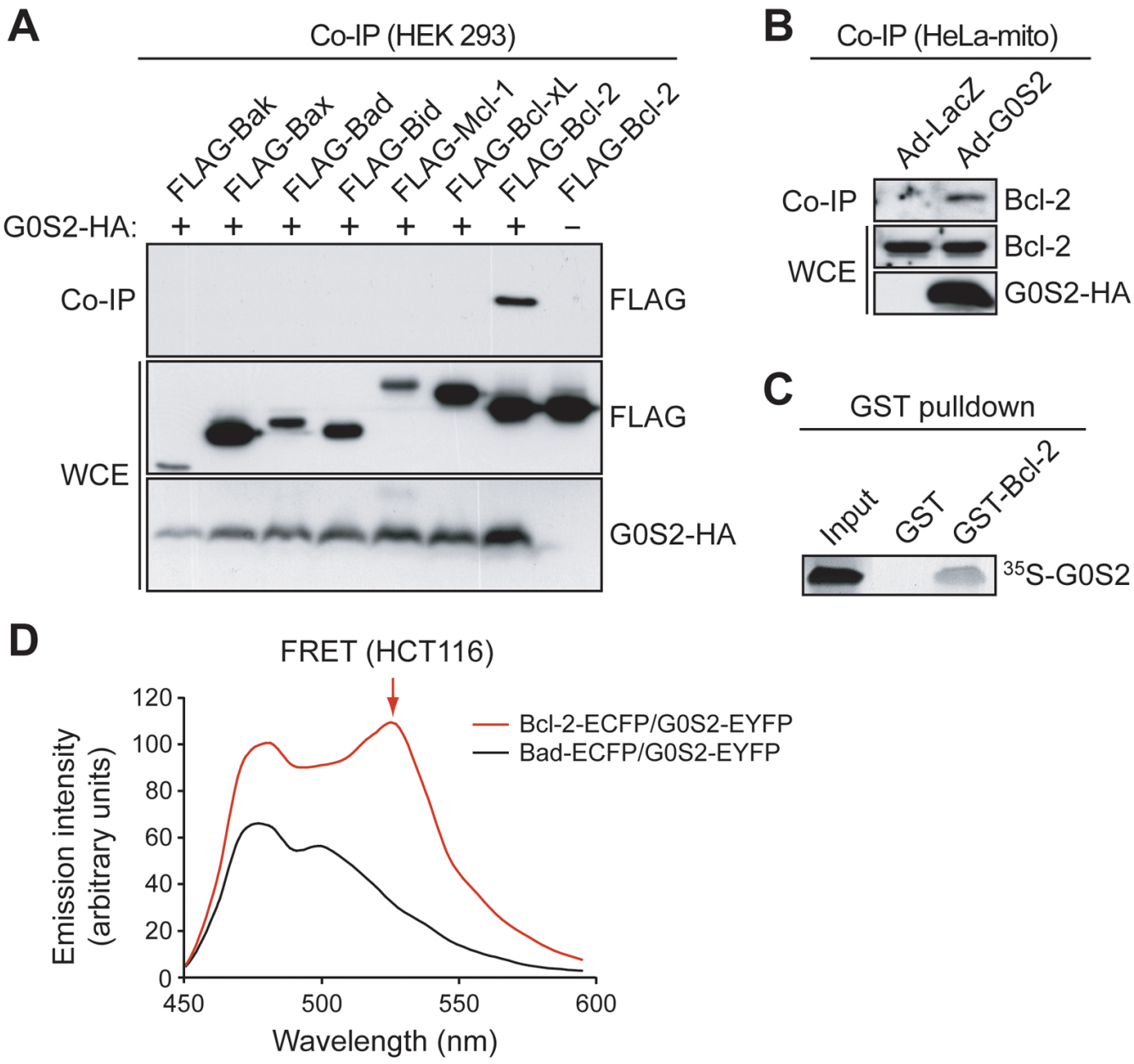

Figure 2.

G0S2 directly interacts with the anti-apoptotic protein Bcl-2. *A*, HEK293 cells were co-transfected with plasmids expressing G0S2-HA and a FLAG-tagged Bcl-2 protein. G0S2 was immunoprecipitated using an α-HA antibody, and the immunoprecipitate was analyzed by immunoblotting with an α-FLAG antibody. The presence G0S2 and Bcl-2 member were also monitored in the whole cell extract (WCE). *B*, G0S2 was immunoprecipitated from the mitochondrial fraction of Ad-G0S2- or Ad-LacZ-infected HeLa cells using an α-HA antibody, and the immunoprecipitate was analyzed using an α-Bcl-2 antibody. *C*, GST pull-down assays using purified GST-tagged Bcl-2 and ^{35}S-methionine labeled G0S2. *D*, FRET analysis. Fluorescence emission spectra in HCT116 cells co-expressing G0S2-EYFP and either Bcl-2-ECFP or Bad-ECFP. The peak of fluorescence emission at 525 nm (FRET signal) is indicated by the arrow.

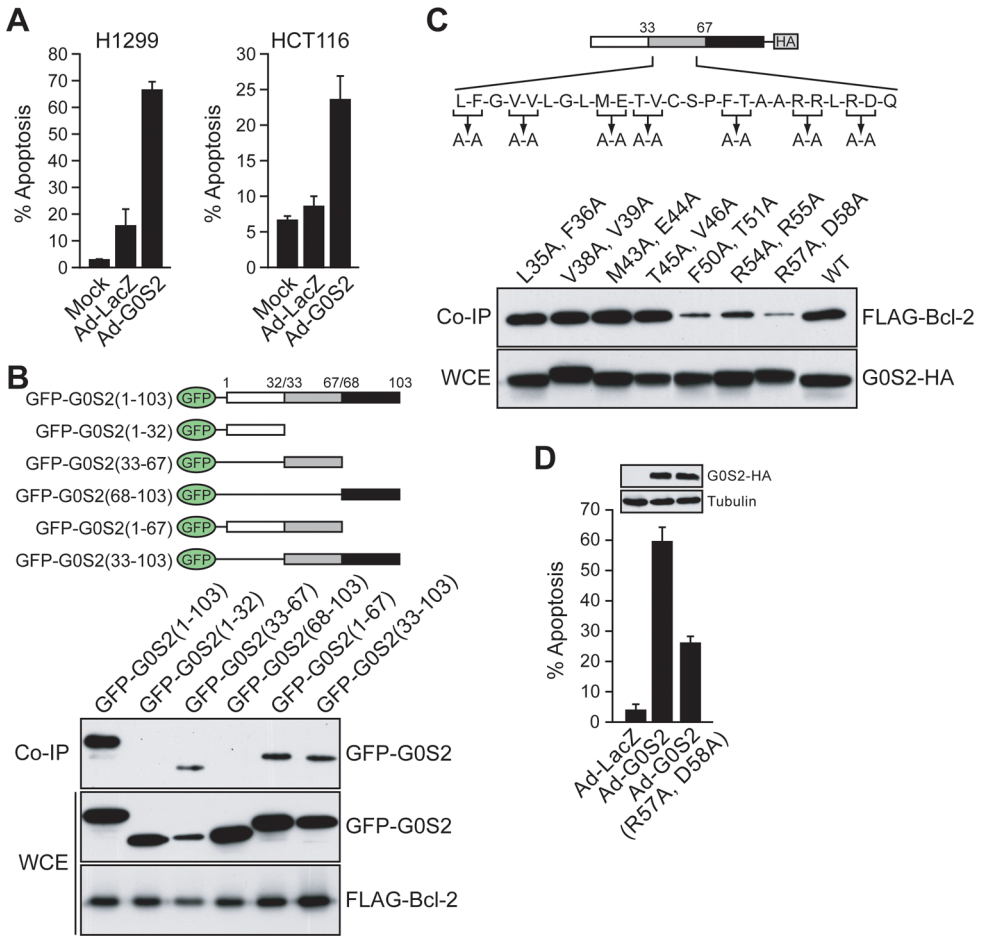

Figure 3.

G0S2 induces apoptosis in transformed cells dependent upon interaction with Bcl-2. *A*, H1299 and HCT116 cells were infected with Ad-G0S2 or Ad-LacZ, or mock-infected, and cell death was monitored by Annexin V-PE staining. *B*, (Top) Schematic representations of GFP-tagged G0S2 deletion mutants. (*Bottom*) H1299 cells were co-transfected with plasmids expressing FLAG-Bcl-2 and GFP-tagged G0S2 deletion mutants. Bcl-2 was immunoprecipitated with an α-FLAG antibody and the immunoprecipitate analyzed with an α-GFP antibody. Also shown are the levels of GFP-tagged G0S2 and FLAG-Bcl-2 in WCE. *C*, (Top) Schematic diagram showing point mutations constructed in the central region of G0S2. (*Bottom*) H1299 cells were co-transfected with plasmids expressing FLAG-Bcl-2 and an HA-tagged G0S2 deletion mutant. G0S2 was immunoprecipitated with an α-HA antibody and the immunoprecipitate analyzed with an α-FLAG antibody. *D*, Apoptosis assays. H1299 cells were infected with Ad-LacZ, Ad-G0S2 or Ad-G0S2(R57A, D58A) and monitored for apoptosis. (*Inset*) Immunoblot showing the G0S2 mutant was expressed at levels comparable to the wild-type protein. Error bars indicate SD.

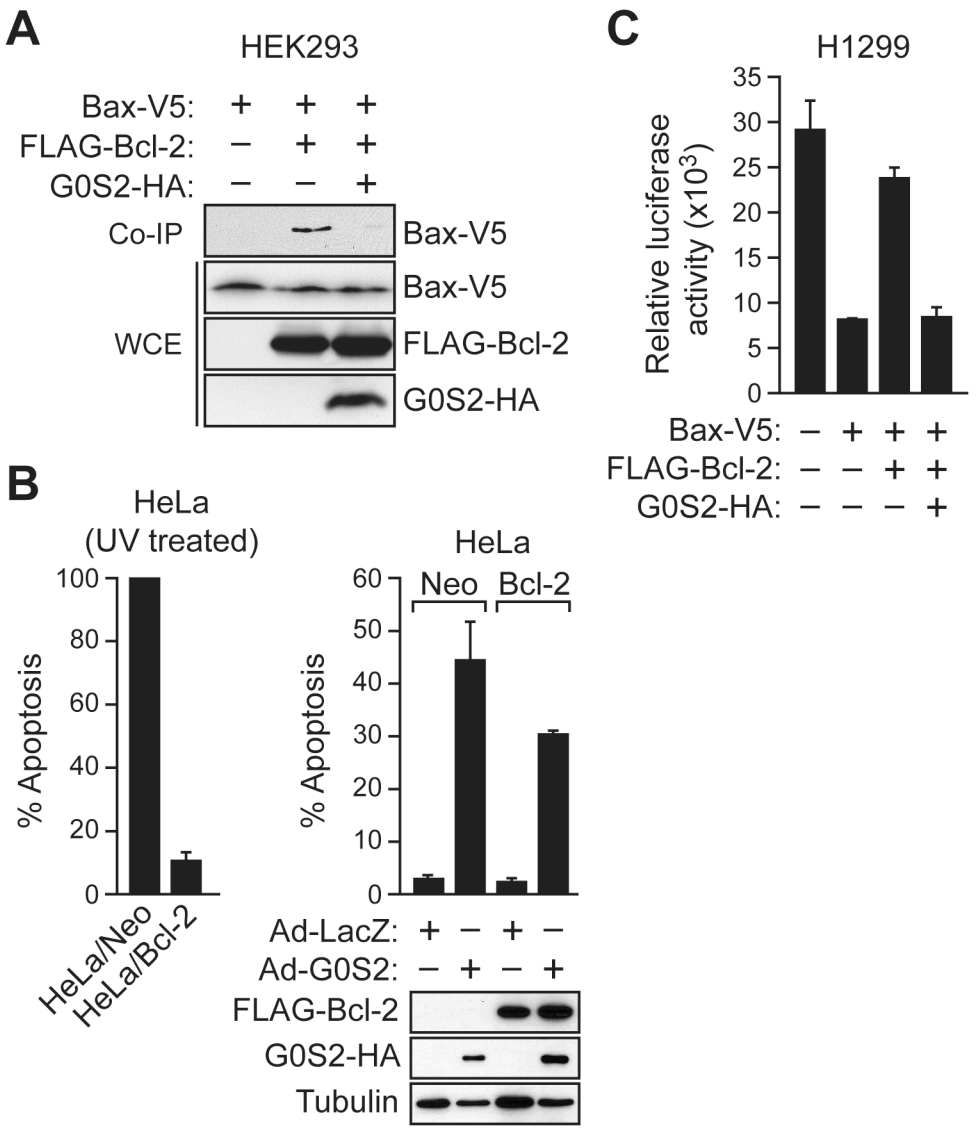

Figure 4.

G0S2 promotes apoptosis by preventing Bcl-2/Bax heterodimerization. *A*, HEK293 cells were co-transfected with plasmids expressing G0S2-HA, FLAG-Bcl-2 and/or V5-Bax. Bcl-2 was immunoprecipitated with an α-FLAG antibody and the immunoprecipitate analyzed with an α-V5 antibody. *B*, (Left) HeLa cells stably expressing Bcl-2 or vector (Neo) were treated with UV. (Right, top) HeLa/Bcl-2 and HeLa/Neo cells were infected with Ad-LacZ or Ad-G0S2, and monitored for apoptosis 48 hours later. (Right, bottom) Immunoblot analysis monitoring expression of Bcl-2, G0S2 and tubulin. *C*, H1299 cells were co-transfected with plasmids expressing luciferase and Bcl-2, Bax and/or G0S2. Luciferase activity was quantified and expressed relative to the levels observed in untransfected cells. Error bars represent SD.

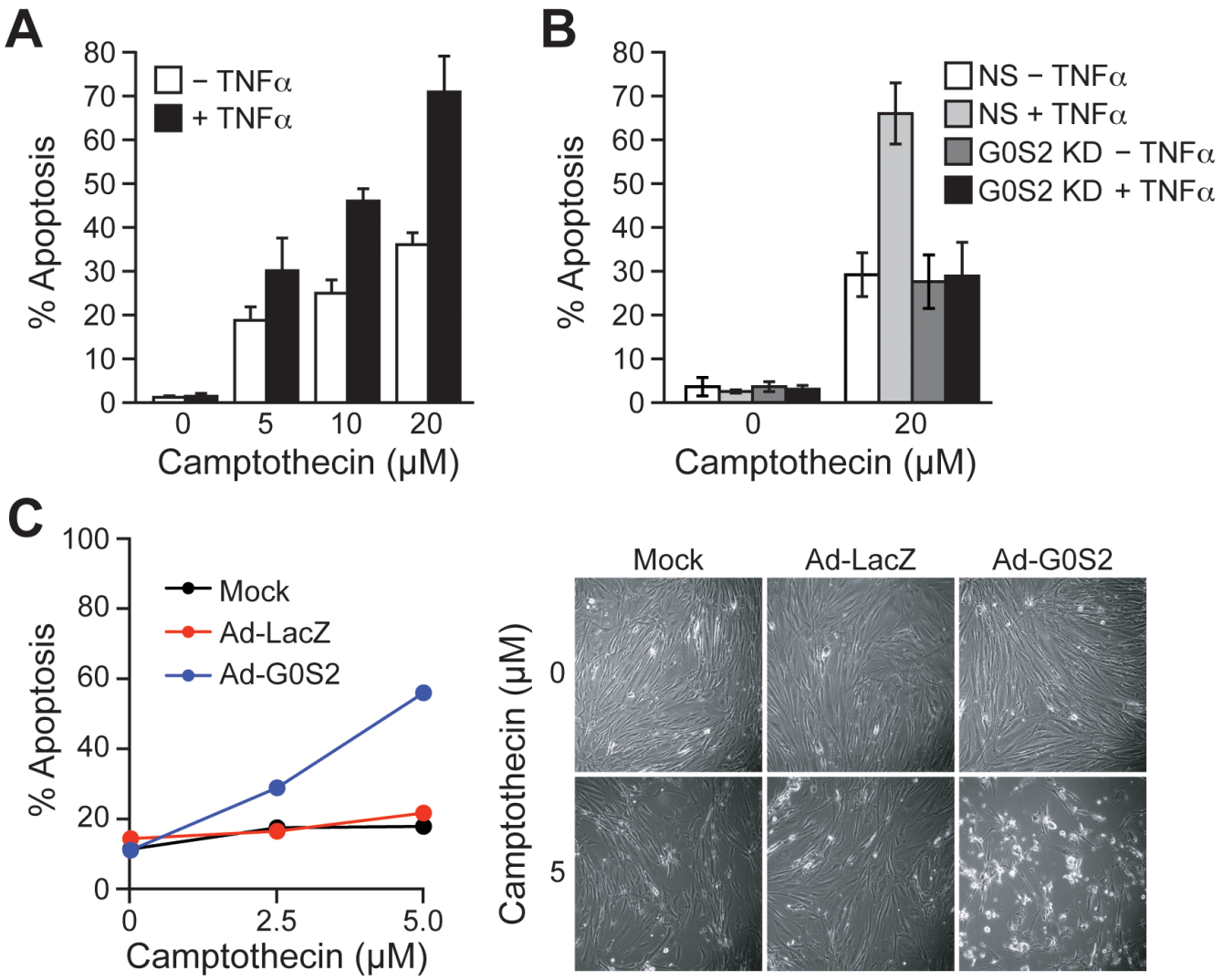

Figure 5.

Ectopic expression of *G0S2* sensitizes primary cells to apoptosis. *A*, PFFs were treated with various concentrations of camptothecin in the presence or absence of TNFα, and monitored for apoptosis. *B*, PFFs stably expressing a non-silencing (NS) or G0S2 shRNA were treated with camptothecin in the presence or absence of TNFα, and monitored for apoptosis. *C*, Mock-, Ad-LacZ-o r A d-G0S2-infected PFFs were treated with various concentrations of camptothecin, and cell death was quantified by Annexin V staining (left) (Right), micrographs. Errors bars represent SD.

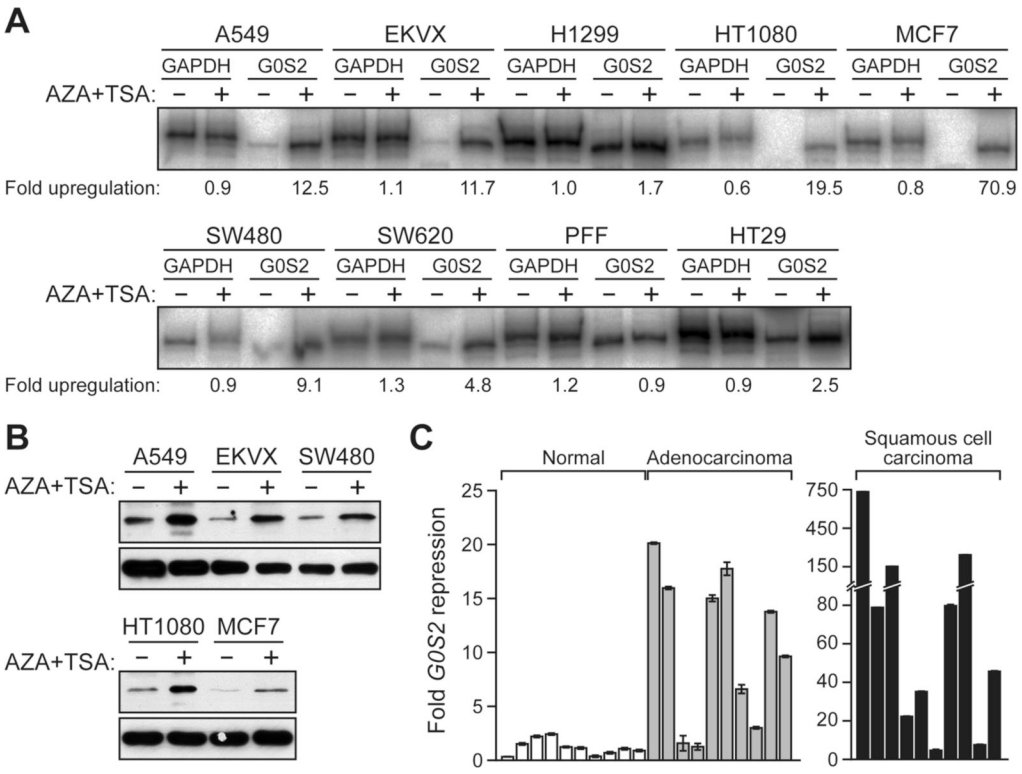

Figure 6.

G0S2 is epigenetically silenced in human cancer cell lines. *A*, RT-PCR analysis of *G0S2* expression in human cancer cell lines and PFFs, in the presence or absence of AZA/TSA treatment. *B*, Immunoblot analysis in a subset of cell lines. *C*, qRT-PCR analysis of *G0S2* expression in 10 individual human normal, adenocarcinoma and squamous cell carcinoma samples. Error bars represent SD.